

# Monogamy and ground-state entanglement in highly connected systems

Alessandro Ferraro, Artur García-Saez, and Antonio Acín

*ICFO-Institut de Ciències Fòniques, Mediterranean Technology Park, 08860 Castelldefels (Barcelona), Spain*

(Received 10 January 2007; revised manuscript received 28 September 2007; published 21 November 2007)

We consider the ground-state entanglement in highly connected many-body systems consisting of harmonic oscillators and spin-1/2 systems. Varying their degree of connectivity, we investigate the interplay between the enhancement of entanglement, due to connections, and its frustration, due to monogamy constraints. Remarkably, we see that in many situations the degree of entanglement in a highly connected system is essentially of the same order as in a low connected one. We also identify instances in which the entanglement decreases as the degree of connectivity increases.

DOI: [10.1103/PhysRevA.76.052321](https://doi.org/10.1103/PhysRevA.76.052321)

PACS number(s): 03.67.Mn, 03.65.Ud, 05.30.-d, 05.50.+q

## I. INTRODUCTION

Entanglement theory has experienced an impressive development in the last decade, mainly due to the key role quantum correlations play in quantum information science. The novel concepts and mathematical methods developed in this new research area are beginning to reveal their usefulness also in different contexts. A striking example of this tendency is given by the physics of quantum many-body systems. As an instance, the analysis of the role played by entanglement in quantum phase transitions allowed for a deeper understanding of this purely quantum phenomenon [1–3]. In this scenario, entanglement theory is also giving a fundamental contribution to the development of new methods capable of simulating efficiently strongly interacting systems [4–6].

Clearly, the correlations between different parts of a many-body system originate from their mutual interaction. In this sense it is natural to expect that the ground state of a strongly interacting and connected quantum system will exhibit a high degree of entanglement. However, this intuition has to be taken cautiously, since the shareability properties of quantum correlations are especially nontrivial and without a classical analog. One of the main differences between classical and quantum correlations is the so-called monogamy of the latter [7]. In the classical scenario, the fact that two systems share some correlations does not prevent them from being correlated with a third party. On the contrary, two maximally entangled quantum systems can share no correlation at all with a third one. More generally, quantum correlations are not infinitely sharable, and the more the entanglement, the smaller the number of systems with which it can be shared.

Consider two similar Hamiltonians consisting of the same interacting terms between a pair of particles, the only difference being the degree of connectivity. One of them, for instance, has only nearest-neighbor interactions, while the second has also next-nearest-neighbor interactions. Let us focus on the ground-state entanglement between two halves of the system. Naively, the more connected Hamiltonian is expected to have a larger entanglement, since there are more bonds connecting the two halves. However, in the more connected system, each particle has to share the quantum correlations with a larger number of particles, so the connecting

bonds may give a smaller amount of entanglement. Therefore, it is unclear which geometry leads to a larger ground-state entanglement.

In this work we analyze the interplay between the enhancement of the ground-state entanglement due to connections and its suppression due to monogamy constraints. We consider spin-1/2 and infinite-dimensional (harmonic oscillators) systems of various geometries with two-body interactions and focus on the bipartite entanglement between two halves of the system. Remarkably, we see that in many situations the degree of entanglement in a highly connected system is essentially of the same order as in the case of a low connected one. Actually, we can even individuate systems for which the entanglement decreases as the degree of connectivity increases.

Before proceeding, let us mention that there exist some works studying how the monogamy of entanglement affects the ground-state properties of Hamiltonians with nearest-neighbor interactions; see, for example, [8,9]. The ground-state entanglement of a highly symmetric and connected system, the so-called Lipkin-Meshkov-Glick model, was also computed in [10].

This paper is organized as follows. In the next section we will introduce the systems we are going to analyze, in particular recalling known results about entanglement calculations in the different cases considered. Then, in Sec. III, we will show in detail how the entanglement depends on the connectivity of the systems themselves. In order to individuate a general behavior we will consider a variety of different connectivity conditions. Specifically, we will analyze both regular and random graph configurations, paying particular attention to the case of bipartite graphs. The relationship between our findings and related results in the context of entanglement-area laws will be outlined in Sec. IV. Even if a way to quantify the action of monogamy in a multipartite setting is still lacking, we will see in Sec. V that the analysis of bipartite monogamy inequalities can shed some light onto our findings. We will close the paper in Sec. VI by discussing possible implications of our findings, in particular in the context of classical simulations of quantum systems.

## II. SPIN AND BOSONIC MODELS

As said, we consider two paradigmatic systems: namely, interacting spin-1/2 and bosonic particles. Concerning the

former, we study a system of  $n$  spin-1/2 particles under the XX Hamiltonian

$$H = \sum_{i,j} t_{ij} [\sigma_x^i \otimes \sigma_x^j + \sigma_y^i \otimes \sigma_y^j], \quad (1)$$

where  $\sigma_k^i$  ( $k=x,y,z$ ) denote the Pauli matrices referred to the  $i$ th particle. The coupling  $t_{ij}$  will be set different from zero when the  $i$ - $j$  couple directly interacts—i.e., in dependence on the topology and connectivity of the system. The actual value of the nonzero  $t_{ij}$  will be chosen randomly, in order to have averaged properties and avoid the dependence of our results on the details of the interaction. Interactions of the type (1) may model highly connected physical systems, such as quantum spin glasses [11]. The entanglement between two parts of the system will be measured by the entropy of entanglement  $E$ : namely, the von Neumann entropy  $S(\rho) = -\text{Tr}[\rho \log_2 \rho]$  of one of the reduced subsystems [12].

Concerning the bosonic case, we consider systems consisting of  $n$  harmonic oscillators with quadratic coupling. Such systems may model discrete versions of Klein-Gordon fields, or vibrational modes in crystal lattices, ion traps, and nanomechanical oscillators. We define the vector  $R$  of quadrature operators by  $R_j = \hat{X}_j$  and  $R_{n+j} = \hat{P}_j$  ( $1 \leq j \leq n$ ), where  $\hat{X}_j$  and  $\hat{P}_j$  are the position and linear momentum operators, respectively. For simplicity, we consider only a coupling via the different position operators, in which case the Hamiltonian is of the form

$$\hat{H} = R^T \begin{pmatrix} V/2 & 0 \\ 0 & \mathbb{1}_{n/2} \end{pmatrix} R, \quad (2)$$

where  $\mathbb{1}_n$  denotes the  $n \times n$  identity matrix. The potential matrix  $V$  is defined via the harmonic coupling between oscillator  $i$  and  $j$ : namely,  $\alpha(\hat{X}_i - \hat{X}_j)^2/2$ . For each geometry considered in the following, we denote by  $C$  the  $n \times n$  adjacency matrix of the corresponding graph, with elements  $c_{ij} = c_{ji} = 1$  if the  $i$ th and  $j$ th oscillators are coupled and  $c_{ij} = c_{ji} = 0$  otherwise. Then, the potential matrix  $V$  is given by  $V_{ij} = -\alpha c_{ij}$  ( $i \neq j$ ) and  $V_{ii} = 1 + \alpha \sum_j c_{ij}$ . The ground state of the system is a Gaussian state characterized by the covariance matrix  $\gamma = (\gamma_x \oplus \gamma_p)/2$ , with  $\gamma_x = V^{-1/2}$  and  $\gamma_p = V^{1/2}$  [13]. We use as entanglement measure the logarithmic negativity [14]  $N_l$  between two generic group  $A$  and  $B$ . It can be shown that  $N_l$  is given by [13]

$$N_l = - \sum_{j=1}^n \log_2 \min[1, \Lambda_j(\gamma_x P \gamma_p P)], \quad (3)$$

where  $\Lambda_j(M)$  is the  $j$ th eigenvalue of the matrix  $M$ . We denote by  $P$  the  $n \times n$  diagonal matrix with  $j$ th diagonal entry given by 1 or  $-1$ , depending on whether the oscillator on position  $1 \leq j \leq n$  belongs to group  $A$  or  $B$ , respectively.

### III. ENTANGLEMENT IN DIFFERENT TOPOLOGIES

#### A. Neighbor coupling

The first configuration that we consider is a one-dimensional (1D) chain of  $n$  particles, in which each of them

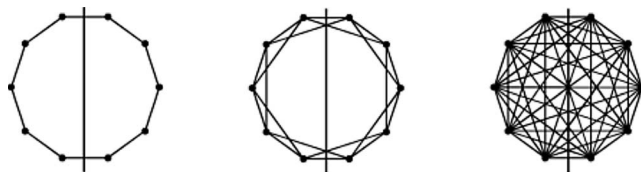


FIG. 1. Closed chain of  $n=10$  interacting particles in the nearest-neighbor ( $n_c=1$ , left), next-nearest neighbor ( $n_c=2$ , center), and fully connected configuration ( $n_c=5$ , right). The entanglement is computed between two halves of the system.

can interact with  $n_c$  of its neighbors on each side. Thus,  $n_c$  is the parameter that characterizes the degree of connectivity in this setting (see Fig. 1). We consider a distance-independent interaction, in order to avoid any dependence on the particular scaling of the interaction strength. In particular, given the ground state, we calculate the entanglement between the two halves of the system (groups  $A$  and  $B$ ) as a function of the number of interacting neighbors  $n_c$ . The typical behavior in the case of a XX system is reported in Fig. 2 for the case of  $n=22$  spins. The exact calculation of the ground state was performed using the SPINPACK package [15]. The solid line represents the averaged ground-state entanglement, where the Hamiltonian parameters  $t_{ij}$  between pairs of particles are randomly chosen in the interval  $[0,1]$ , while the dashed line gives the largest entanglement obtained. We clearly see that the entanglement grows only slightly and, in particular, the fully connected chain has a degree of entanglement comparable to the nearest-neighbor coupled chain. Note that, by contrast, the number of bonds connecting the two halves of the chain increases as  $n_c^2$ . The same behavior has been observed for different Hamiltonian operators, consisting of other interaction terms, and smaller sizes.

We consider now the same configuration for the case of a chain of harmonic oscillators. As said above, the interactions between the particles simply correspond to oscillators of coupling constant  $\alpha$ . The entanglement between the two halves of an open chain consisting of  $n=100$  oscillators is shown in the inset of Fig. 2, where the logarithmic negativity

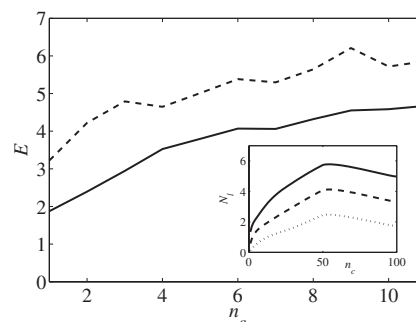


FIG. 2. For a closed chain of  $n=22$  spin-1/2 particles with XX interaction (1), the entropy of entanglement is plotted versus the number of connected neighbors,  $n_c$ , averaged over 100 realizations. The dashed line gives the largest entanglement obtained. Inset: for an open chain of  $n=100$  oscillators the logarithmic negativity  $N_l$  is plotted versus  $n_c$ . From top to bottom the coupling constant  $\alpha$  is given by  $\alpha=10, 1, 0.1$ .

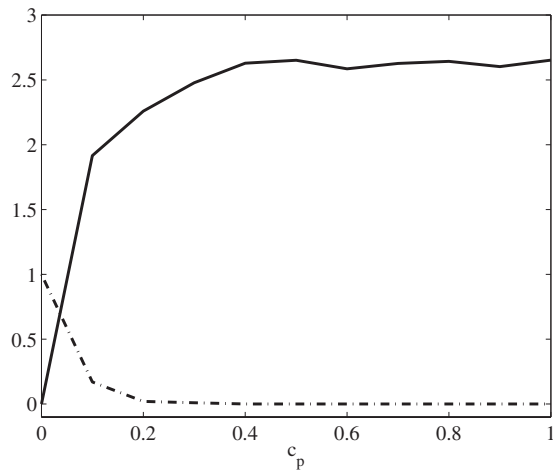


FIG. 3. Entropy of entanglement for a randomly coupled system with  $n=10$  spins (solid), its degeneracy (dash-dotted line) and its energy (dashed line), as a function on  $c_p$ . We averaged over 100 executions.

is plotted versus the number of coupled neighbors,  $n_c$ . One clearly see that the entanglement increases (almost linearly) as far as  $n_c \lesssim n/2$ , whereas for higher connected systems the entanglement is frustrated. The frustration mechanism is indeed stronger than in the spin case, the entanglement decreasing at some point as the number of connections increases. Notice the quite universal behavior of these curves: the position of the maximum does not depend on the coupling constant  $\alpha$ , and as one can expect, the entanglement increases with  $\alpha$ , for fixed  $n_c$ .

Both examples reported here confirm that the monogamy of entanglement plays a predominant role for highly connected systems. As said, as the connectivity increases, each particle of, e.g., set  $A$  becomes as well entangled with many other particles of the same set. This in turn limits, for monogamy reasons, entanglement with particles of set  $B$ .

### B. Random coupling

We have seen above that the details of the entanglement frustration mechanism depend on the system under consideration; nevertheless, the general behavior is the same for a variety of situations. As another example, particularly different from the 1D chain above, consider now a random configuration in which each couple of particles  $i$  and  $j$  is connected with probability  $c_p$ , which will be called the connectivity parameter. Then, the connections are given by the edge of a graph with random (symmetric) adjacency matrix. Concerning the case of the  $XX$  system, the typical behavior is reported in Fig. 3, where the entropy of entanglement is plotted as a function of the connectivity parameter. We also plot the degeneracy of the ground state. Indeed, if the degeneracy was nonzero for a significant range of values of  $c_p$ , the results should be carefully considered, since there may be other ground states having quite different entanglement properties. However, this does not affect the validity of our results, since the degeneracy is equal to zero already for small values of the connectivity parameter. Actually, this de-

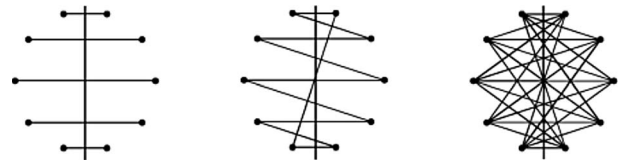


FIG. 4. Regular bipartite graph of  $n=10$  interacting particles for increasing connectivity.

generacy disappears for values of  $c_p$  close to  $n/n_t$  (where  $n_t$  is the number of connections of the complete graph)—i.e., when we are able to construct a connected graph with high probability. In general, we see again that the entanglement saturates and the saturation value is reached for a low value of the connectivity, showing again the strong effect of monogamy.

In the case of bosonic oscillators, one also retrieves the general behavior already highlighted in the previous configuration. Namely, the entanglement increases up to a certain value of the connectivity parameter ( $c_p$  in the present configuration), after which the monogamy constraint starts causing a decrease of the entanglement.

### C. Bipartite graphs

We exploit now the configuration in which perhaps the effects of monogamy show up more impressively: namely, the case in which the system can be represented by a bipartite graph. The latter is constituted by two sets  $A$  and  $B$  for which particles belonging to the same set do not directly interact (see Fig. 4). Then, *a priori*, one could expect that in such a configuration the effects of monogamy should be weaker than in the configurations discussed above. We report here the results for both regular and random bipartite graphs in the case of harmonic oscillators.

Let us first consider the case of a random bipartite graph. As above, we name connectivity parameter  $c_p$  the probability that a generic particle in  $A$  interacts with a particle in  $B$ . For example, in the fully connected case ( $c_p=1$ ) each particle in  $A$  is coupled to all the particles in  $B$ . For a fixed coupling constant we look for the optimal  $c_p^{\text{opt}}$  such that the entanglement is maximized. As shown in Fig. 5, we have that  $c_p^{\text{opt}} \neq 1$  in general, depending nontrivially on  $\alpha$ . Namely, for large values of  $\alpha$  the maximum entanglement is provided by a Hamiltonian with few connections for each oscillator. Vice versa, for low values of  $\alpha$  the completely connected case tends to maximize the entanglement. Note again that particles belonging to the same set do not directly interact. However, these particles become entangled through a common interaction with particles of the other set. This, at the same time, limits the amount of entanglement between the two sets because of monogamy.

In order to obtain a deeper insight into the behavior described above, let us now consider a regular graph. In this case, remarkably, it is straightforward to obtain an explicit expression of the log-negativity for an arbitrary large number of particles. Let us focus on a periodic system consisting of  $n$  oscillators (labeled from 1 to  $n$ ) and consider two sets composed such that the even oscillators belong to  $A$  and the odd

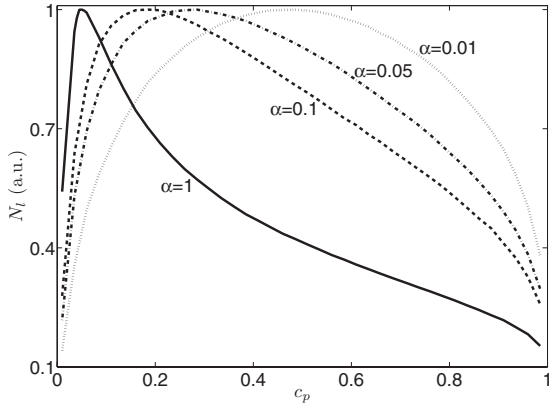


FIG. 5. For a random bipartite graph of harmonic oscillators the logarithmic negativity  $N_l$  is plotted (normalized for each  $\alpha$ ) versus the connectivity parameter  $c_p$  for different coupling constants  $\alpha$ . The total number of particles is  $n=100$ .

ones to  $B$ . If each oscillator in set  $A$  interacts only with  $2n_c$  oscillators in  $B$  [specifically, the  $(2j)$ th oscillator interacts with oscillators labeled  $2k+1$  with  $k=j-n_c, \dots, j+n_c$ ], then the interaction matrix  $V$  in Eq. (2) is given by a circulant matrix  $V_{bg}$ , whose first row is given by the vector

$$\mathbf{v} = (1 + 2\alpha n_c, \underbrace{-\alpha, 0, \dots, -\alpha, 0, 0, \dots, 0, 0}_{n_c \text{ times}}, \underbrace{0, 0, \dots, 0, -\alpha, \dots, 0, -\alpha}_{n_c \text{ times}}). \quad (4)$$

The eigenvalues of  $V_{bg}$  are given by

$$\lambda_k = 1 + 2\alpha n_c - 2\alpha \sum_{j=1}^{n_c} \cos\left[(2j-1)k \frac{2\pi}{n}\right]; \quad (5)$$

hence, following Ref. [13], the log-negativity between sets  $A$  and  $B$  can be straightforwardly obtained:

$$N_l = \frac{1}{2} \sum_{k=0}^{n/2-1} \left| \log_2 \frac{\lambda_k}{\lambda_{n/2-k}} \right|. \quad (6)$$

When  $n$  is large, the sum above turns into a Riemann series, which gives an explicit expression for the log-negativity:

$$N_l \approx \frac{n}{4\pi} f(\alpha, n_c), \quad (7)$$

where we have defined the function

$$f(\alpha, n_c) = \int_0^\pi dx \left| \log_2 \left\{ 1 + 2\alpha n_c - 2\alpha \sum_1^{n_c} \cos[(2j-1)x] \right\} \right. \\ \left. - \log_2 \left\{ 1 + 2\alpha n_c - 2\alpha \sum_1^{n_c} \cos[(2j-1)(\pi-x)] \right\} \right| \quad (8)$$

in order to single out the dependence on  $\alpha$  and the connectivity parameter  $n_c$ . Noticeably, in Eq. (7) the dependence on  $n$  factorizes, allowing us to analyze how the connectivity affects the entanglement by simply looking at  $f(\alpha, n_c)$  for different coupling regimes (see Fig. 6). It can be seen that the

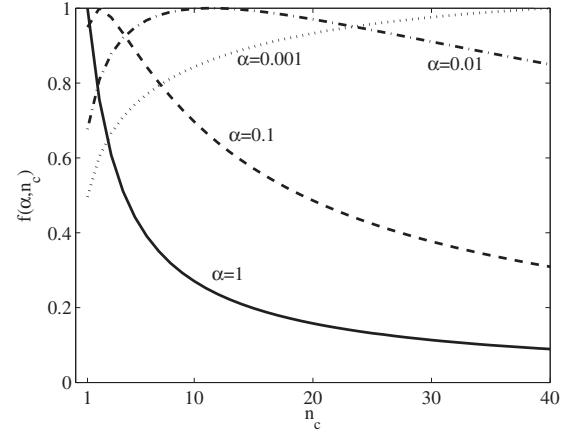


FIG. 6. For a regular bipartite graph of harmonic oscillators the function  $f(\alpha, n_c)$  in Eq. (8) is plotted versus the connectivity parameter  $n_c$  (arbitrary units, normalized for each  $\alpha$ ) for different coupling constants  $\alpha$  (see text for details).

results are very similar to the ones of a random bipartite graph, indicating that the asymmetries of the latter do not play a significant role. As in Fig. 5, for weak coupling the entanglement increases with the connectivity of the system, meaning that monogamy does not play a significant role. On the other hand, for strong coupling the entanglement suddenly decreases with  $n_c$ . This is a clear sign of the action of monogamy constraints, since for high values of  $\alpha$  a high degree of entanglement is created already for small  $n_c$ .

#### IV. CONNECTIVITY AND AREA LAW

In this section we want to elucidate the relation between the findings exposed above and the general issue concerning entanglement-area laws. A number of theoretical investigations have shown that, for a variety of physical systems, the entanglement between two complementary regions scales as the area between them [16]. For instance, it is shown in Refs. [3,17] that, for noncritical systems with nearest-neighbor coupling, the entanglement between a distinguished part of a system and the rest increases as the number of connections. Regarding more general interactions, in particular long-range ones, the boundary area (given by the connections between the two regions of the system) only gives an upper bound to the entanglement [18]. In all these works the Hamiltonian of the global system is kept fixed, whereas the size of the distinguished region varies. It is then clear that the monogamy constraints do not act significantly, since the connectivity of the systems remains unchanged with size. On the contrary, in most of our previous analyses we kept fixed the size of the distinguished region, whereas the connections between particles were modified by changing the degree of connectivity of the Hamiltonians (see Figs. 2, 3, and 5).

Following an approach suitable for a comparison with the works on area laws, we exploited also the dependence of the entanglement on the size of the system. The results are reported in Fig. 7, where the main panel refers to the case of an  $XX$  spin system and the inset to a harmonic one. In both cases we considered the nonrandom configuration exploited

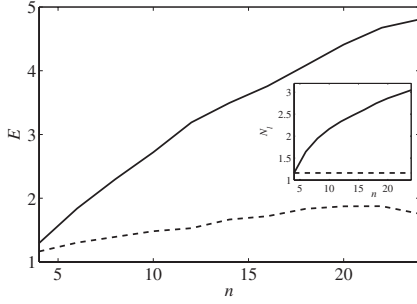


FIG. 7. For an  $XX$  spin system the entropy of entanglement  $E$  between the two halves of the system is plotted as a function of the system size  $n$  (averaged over 100 realizations). Inset: corresponding graph for the negativity  $N_l$  in a closed harmonic chain with  $\alpha=1$  for nearest-neighbor coupling (dashed line) and optimal coupling (solid line; see text).

in Sec. III A. In particular, we focused on the results corresponding to (i) nearest-neighbor coupling and (ii) the optimal configuration in which the number of connections,  $n_c$ , is chosen in order to give the maximal amount of entanglement. For a closed harmonic chain, we observe that the entanglement remains constant in the nearest-neighbor case (as we expect from the results of Ref. [13]), whereas it increases only logarithmically in the optimally connected case. Actually, an exact logarithmic increase can be derived in a fully connected topology (i.e.,  $n_c=n$ ), for which the computation of the log-negativity is straightforward following again Ref. [13]. There, a lower bound to the log-negativity is given as a function of the coupling parameters. Fortunately, such a bound turns out to be tight in the case of both nearest-neighbor and fully connected systems [19]. In particular, for the latter the log-negativity is given by

$$N_l = \frac{1}{2} \log_2[1 + 2n\alpha], \quad (9)$$

proving a logarithmic increase with  $n$ . Remarkably, the behavior is similar for a closed spin chain, as can be seen in Fig. 7. Recall that in this case the optimal number of connections  $n_c^{\text{opt}}$  is always given by  $n_c^{\text{opt}}=n$ , as pointed out in Sec. III A. Although our computations are not very conclusive, they suggest a sublinear increase in this case too.

As said, the scenario in Fig. 7 is suitable for a comparison with the works concerning area laws, in particular the ones dealing with half spaces (see, e.g., Ref. [20]). We see that, as expected, for nearest-neighbor interactions an entanglement-area law is satisfied (since we are not dealing with critical systems). On the contrary, the slight entanglement increase for highly connected systems strongly contrasts with the increase of the number of bonds linking the two halves of a chain, which scales as  $(n/2)^2$ . As recalled, in these cases the boundary area only gives an upper bound for the entanglement. Thus, our results reveal that the entanglement can actually scale sensibly slower than the area in highly connected systems.

## V. MONOGAMY INEQUALITIES

To quantify how the monogamy of entanglement acts in the analyzed scenarios we can refer to monogamy inequalities. In particular, for the case of harmonic oscillators we considered the inequality introduced in Ref. [21], where the Gaussian tangle  $\tau$  is used as entanglement measure. We recall that the latter is defined as the square of the negativity, for pure states, and then extended to mixed states via a convex roof. In particular, the monogamy constraint for  $n$  modes can be expressed as

$$\tau^{1:2,\dots,n} \geq \sum_{j=2}^n \tau_1^{1:j}, \quad (10)$$

where  $\tau^{1:2,\dots,n}$  denotes the tangle between the first mode and the remaining ones, whereas  $\tau_1^{1:j}$  is the two-mode tangle between the first mode and the  $j$ th one. The difference between the left- and right-hand sides of Eq. (10) is called residual entanglement, and it indicates the presence of a complex structure of the quantum correlations, not simply ascribable to two-mode entanglement.

The results are reported in Fig. 8 for bosonic oscillators in a regular bipartite graph (see Sec. III C). We see that when the residual entanglement begins to be comparable to the sum of the two-mode tangles, then the entanglement between sets  $A$  and  $B$  starts to be suppressed. In other words, when a complex entanglement structure appears, then particles belonging to the same set start to become quantum correlated. As a consequence of monogamy, they can then share no longer a high amount of correlations with the particles belonging to the other set and the bipartite entanglement between  $A$  and  $B$  is suppressed. Notice that as the strength of the coupling between the oscillators increases, the effects of monogamy become more and more important, as one may expect by general considerations. The additional frustration in proximity to the fully connected graph can be instead attributed to symmetric reasons. More specifically, in a fully connected graph the state of the system is completely symmetric, which in turn implies a reduction of the effective size of the Hilbert space associated with the  $n$  oscillators. As a consequence, the entanglement in the system is frustrated too.

For spin systems we considered the monogamy inequality presented in Refs. [7,22] where  $\tau$  is now the square of the concurrence, or tangle, a measure of entanglement between qubits. Figure 9 shows, for the regular bipartite graph with  $n_c$  connected neighbors, the quantities  $\sum_{j=2}^n \tau_1^{1:j}$  and  $\tau^{1:2,\dots,n}$ . For any value of the connectivity, any spin is maximally entangled with the rest, since  $\tau^{1:2,\dots,n}=1$ . However, as the number of connections increases, the structure of entanglement becomes highly nontrivial. This, as said, limits the bipartite entanglement between sets  $A$  and  $B$ . Notice that, due to the absence of an on-site interaction in Eq. (1), an analogy can be seen between the  $XX$  system and the harmonic one in the strong-coupling regime.

## VI. CONCLUSIONS

We have analyzed the interplay between ground-state entanglement and the connectivity in spin-1/2 and bosonic sys-

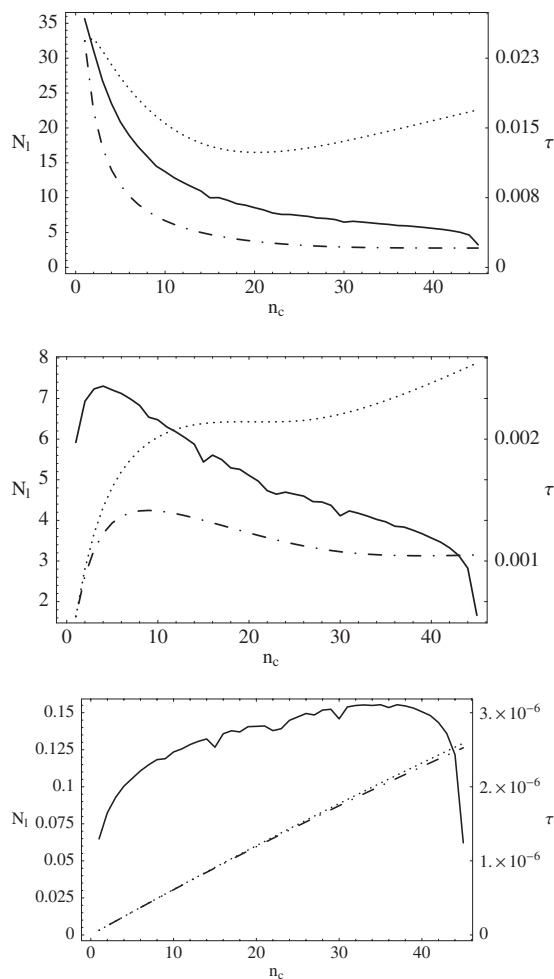


FIG. 8. For a regular bipartite graph of  $n=90$  harmonic oscillators the logarithmic negativity  $N_l$  is plotted versus the number of connections per oscillator  $n_c$  (solid line, left y axis). The dotted and dot-dashed lines are the plot of  $\tau^{1:2,\dots,n}$  and  $\sum_{j=2}^n \tau_l^{1:j}$ , respectively (right y axis). From top to bottom the coupling constant is  $\alpha = 1, 0.1, 0.01$ .

tems with two-body interactions. We have shown that the ground-state entanglement does not necessarily increase by introducing more interacting terms in the Hamiltonian. Actually, for some systems, it does decrease with the number of connections. From a more applied point of view, the amount of entanglement across different bipartitions of a system has

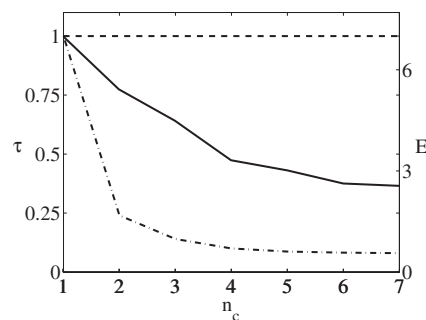


FIG. 9. For a bipartite graph of  $XX$  spin systems with  $n=14$ , the entropy of entanglement,  $E$ , is plotted versus the number of connections,  $n_c$  (solid line, right y axis). The dashed and dot-dashed lines are the plot of  $\tau^{1:2,\dots,n}$  and  $\sum_{j=2}^n \tau_l^{1:j}$ , respectively (left y axis). The average is taken over 100 realizations.

been related to the complexity of the classical description of the state [23]. Although here we just focus on symmetric partitions, it seems reasonable to expect that such partitions have the highest entanglement (among the contiguous ones). Thus, the previous analysis suggests that the bipartite entanglement for many highly connected systems is similar to the one for low connected Hamiltonian systems, where efficient classical algorithms exist, like, for example, the density matrix renormalization group (DMRG). As a matter of fact, the latter method has recently been efficiently applied to a specific highly connected model in order to analyze quantum phase transitions in spin glasses [24]. The efficiency of the DMRG in this scenario is not trivial, and it is related to the fact that the specific system analyzed in Ref. [24] turns out to be only slightly entangled. We have shown here that a large variety of systems may have such a character, due to the fundamental constraint imposed by the monogamy of entanglement. Our results, then, may encourage the search for novel classical algorithms able to simulate highly connected quantum systems.

ACKNOWLEDGMENTS

We acknowledge S. Iblisdir and R. Orús for discussions. This work is supported by the EU QAP project, the Spanish MEC, under Project No. FIS 2004-05639 and the Consolider-Ingenio 2010 QOIT program, the “Ramón y Cajal” and “Juan de la Cierva” grants, the Generalitat de Catalunya, and the Università di Milano under grant “Borse di perfezionamento all’estero.”

[1] A. Osterloh, L. Amico, G. Falci, and R. Fazio, *Nature (London)* **416**, 608 (2002).  
 [2] T. J. Osborne and M. A. Nielsen, *Phys. Rev. A* **66**, 032110 (2002).  
 [3] G. Vidal, J. I. Latorre, E. Rico, and A. Kitaev, *Phys. Rev. Lett.* **90**, 227902 (2003).  
 [4] G. Vidal, *Phys. Rev. Lett.* **93**, 040502 (2004).  
 [5] F. Verstraete, D. Porras, and J. I. Cirac, *Phys. Rev. Lett.* **93**,

227205 (2004).  
 [6] S. Anders, M. B. Plenio, W. Dur, F. Verstraete, and H. J. Briegel, *Phys. Rev. Lett.* **97**, 107206 (2006).  
 [7] V. Coffman, J. Kundu, and W. K. Wootters, *Phys. Rev. A* **61**, 052306 (2000).  
 [8] K. M. O’Connor and W. K. Wootters, *Phys. Rev. A* **63**, 052302 (2001).  
 [9] M. M. Wolf, F. Verstraete, and J. I. Cirac, *Phys. Rev. Lett.* **92**,

- 087903 (2004).
- [10] J. I. Latorre, R. Orus, E. Rico, and J. Vidal, Phys. Rev. A **71**, 064101 (2005); T. Barthel, S. Dusuel, and J. Vidal, Phys. Rev. Lett. **97**, 220402 (2006).
- [11] S. Sachdev, *Quantum Phase Transitions* (Cambridge University Press, Cambridge, England, 1999).
- [12] C. H. Bennett, H. J. Bernstein, S. Popescu, and B. Schumacher, Phys. Rev. A **53**, 2046 (1996).
- [13] K. Audenaert, J. Eisert, M. B. Plenio, and R. F. Werner, Phys. Rev. A **66**, 042327 (2002).
- [14] G. Vidal and R. F. Werner, Phys. Rev. A **65**, 032314 (2002).
- [15] <http://www-e.uni-magdeburg.de/jschulen/spin/>.
- [16] M. Srednicki, Phys. Rev. Lett. **71**, 666 (1993).
- [17] M. B. Plenio, J. Eisert, J. Dreißig, and M. Cramer, Phys. Rev. Lett. **94**, 060503 (2005).
- [18] M. Cramer and J. Eisert, New J. Phys. **8**, 71 (2006).
- [19] This is due to the fact that in both cases the matrix  $V''F$  is semidefinite (see Ref. [13] for details). For the sake of completeness, we recall that  $V''$  is defined by considering the bipartition  $V = \begin{pmatrix} V' & V'' \\ V'' & V' \end{pmatrix}$ , whereas  $F_{i,j} = \delta_{i,n+1-j}$ .
- [20] M. Cramer, J. Eisert, and M. B. Plenio, Phys. Rev. Lett. **98**, 220603 (2007).
- [21] T. Hiroshima, G. Adesso, and F. Illuminati, Phys. Rev. Lett. **98**, 050503 (2007).
- [22] T. J. Osborne and F. Verstraete, Phys. Rev. Lett. **96**, 220503 (2006).
- [23] G. Vidal, Phys. Rev. Lett. **91**, 147902 (2003).
- [24] J. Rodríguez-Laguna and G. E. Santoro, e-print arXiv:cond-mat/0610661.